International Journal of Computer Networking,
Wireless and Mobile Communications (IJCNWMC)
ISSN (P): 2250-1568; ISSN (E): 2278-9448
Vol. 7, Issue 2, Jun 2017, 1-18

TRANS STELLAR
•Journal Publications •Research Consultancy

MITIGATING INTERFERENCE LINKED TO MATERIAL COMPOSITION FOR WIRELESS SENSOR NETWORK DEPLOYMENT IN REAL THREE-DIMENSIONAL INDOOR SPACES

HER-SHING WANG, CHIH-HSING TU & YU-JEN CHIU

Department of Industrial Engineering & Management, National Taipei University of Technology, Taipei, Taiwan

ABSTRACT

In the Industry 4.0 era, traditional manufacturing and other industries must urgently upgrade their production techniques to attain small lot and variable production. How to connect production machines and tools through wireless sensor network (WSN) infrastructure is a key issue.

In general, methods for the deployment of WSNs focus on two-dimensional free space for optimization. In this study, real plants that required a large indoor three-dimensional plant space environment for WSN optimization were simulated. Wireless interference caused by obstructions is an NP-hard problem for large-space network planning.

To investigate interference caused by material composition, we constructed four scenarios with obstructions composed of different materials and used a multiobjective mathematical model for optimization.

We propose a heuristic technique that uses the nondominated sorting genetic algorithm (NSGA-II) to obtain suitable deployment solution sets. The model was empirically proven to reduce interference by changing the material composition of obstruction-causing materials.

KEYWORDS: Three-Dimensional Space, Wireless Sensor Network, Interference Problem, Path Loss & Genetic Algorithm

Received: Feb 24, 2017; **Accepted:** Mar 23, 2017; **Published:** Apr 25, 2017; **Paper Id.:** IJCNWMCJUN20171

Original Article

1. INTRODUCTION

Chang et al. (2009) indicated that because customer-oriented marketing has become a trend, production patterns are characterized by small volumes and wide varieties. Many manufacturers must upgrade their manufacturing technology so that plant equipment and machinery can be linked to attain the desired plant automation level.

Wireless sensors are currently widely applied in various industries. Wireless sensor networks (WSNs) are a type of infrastructure for smart factories in the Industry 4.0 era. Indoor deployment planning for WSNs is vital in three-dimensional (3D) plant spaces. Planning for WSN installation requires considering the following factors: (a) fault tolerance, (b) scalability, (c) cost, (d) hardware constraints, (e) transmission media, (f) environment, (g) sensor network topology, and (h) power consumption. This study investigated real indoor environments that feature different challenges for installing WSNs, including wireless interference arising from obstructions caused by the composition of different materials.

In a 3D indoor environment, achieving full coverage for all wireless sensors in the network is ideal. In a

small space, achieving full coverage is relatively straightforward; however, in larger spaces, WSN deployment is an NP-hard problem. Past studies have focused mainly on two-dimensional (2D) spaces, but the conversion of signal transmission connections and coverage from 2D to 3D spaces is also an NP-hard problem (Younis and Akkaya, 2008). The Z-axis height in real spaces should be a consideration.

On the basis of the aforementioned factors, the present study established a multiobjective mathematical model by using the nondominated sorting genetic algorithm II (NSGA-II) developed by Deb et al. (2002). The objectives of this study were to (a) calculate the optimal WSN reader by using the NSGA-II algorithm, (b) maximum wireless coverage, (c) minimum signal conflict occurrence rate, (d) optimize the deployment locations in a space that features obstructions, and (e) used to establish a practical mathematical model to achieve multiobjective optimization of the feasible solution to replace conventional deployment planning practices.

The multiobjective mathematical model was built into a decision-making system to increase the efficiency of decision-making processes and enhance overall competitiveness.

2. LITERATURE REVIEW

2.1 WSNs Planning in Real 3D Indoor Space

The main advantage of 3D indoor space research is that it considers the complex shapes of objects, such as by evaluating the absolute and relative object height and volume and by mimicking a real environment. This study investigated the material composition of such objects.

Many plants have distinct warehouse and production areas as well as areas for raw materials as well as finished and incomplete products. Packaging materials are generally stored in the warehouse area, whereas assembly and operation lines are located in the production area. A real indoor plant environment is shown in Figure 2.1.

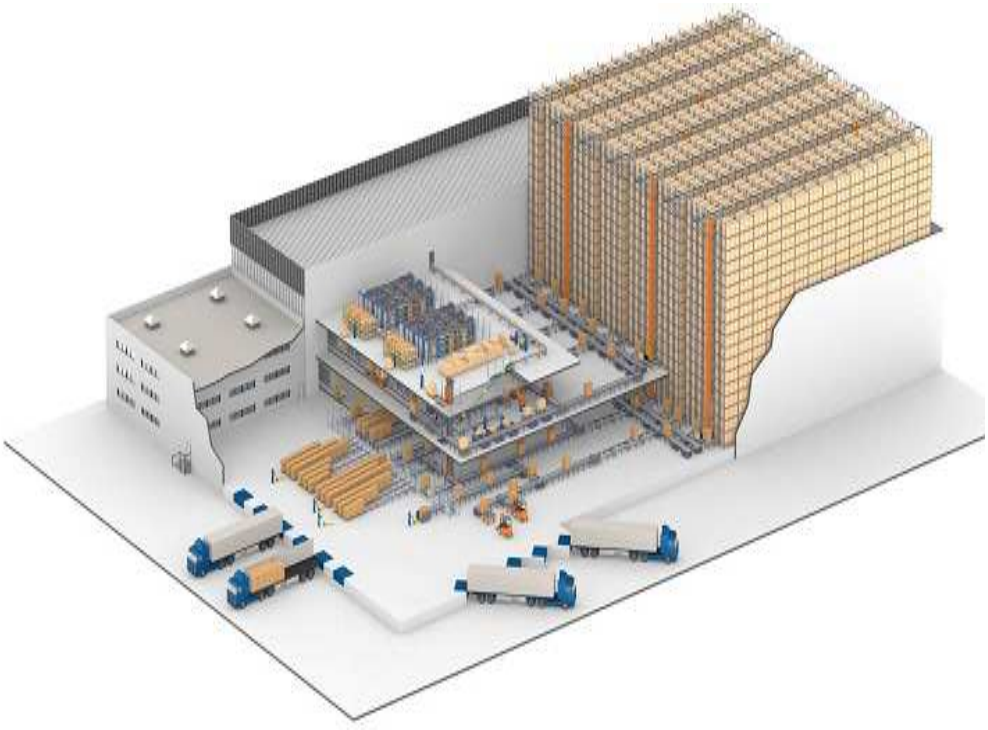

Figure 2.1: Plant Indoor Environment

Conventional manufacturing industries upgrade their manufacturing environment to include a stable, reliable wireless environment. Production equipment, inspection equipment, test equipment, infrared sensors, distance sensors, and RFID pallets in production areas must be connected to wireless infrastructure to record parameters and product information. For 3D indoor wireless signal deployment, assessment indicators include coverage, availability, accuracy, update frequency, cost, and system complexity. (a) Coverage means that all tags can receive the signal ratio. (b) Availability indicates that the strength of the received tag signal must exceed the threshold and the received tag signal is subject to minimal signal interference to avoid affecting usability. (c) Accuracy indicates the error distance of the position. (d) Update frequency indicates the system refresh rate. (e) Cost includes hardware, construction, maintenance, and management costs. (f)System complexity includes wireless component items, quantity, and techniques.

This study investigated these indicators to design a multiobjective and constraint-based model. In contrast to most previous related studies, which have focused on 2D spaces and effect studies (Tao et al., 2015), the present study adopted a real 3D space, almost identical to an actual indoor plant space environment and subject to nearly identical constraints, to plan for WSN implementation. Ko (2010) used the trilateration concept to design a 3D position-sensing algorithm to resolve the issue of target positioning in a 3D space. Despite the results showing a reduction in positioning errors and the calculation times, the algorithm did not compensate for signal weakness or space limitations.

2.2. Wireless Communication Technique

WSN s technology, the standard includes Wi-Fi, RFID, and Bluetooth, and ZigBee, characteristics as (Table 2.1).

Table 2.1: Wireless Communications Standards

Standard	Accuracy	Coverage	Range	Line of sight	Power
WIFI	1 m	Building	10–100 m	NOL	High
Active-RFID	1 m	Building	10–100 m	NOL	Medium
Passive-RFID	0.2 m	Room	1–5 m	Line	Low
Bluetooth	1–2 m	Building	10–30 m	Line/ NOL	Low
ZigBee	2 m	Building	20–30 m	NOL	Low

In the present study, Wi-Fi and RFID were employed to determine the wireless communications parameters for a design based on Ginters and Martin-Gutierrez (2013).

2.3. Wireless Signal Interference Problems

Wireless signal transmissions are easily affected by interference, and various factors may affect the reliability and stability of signal transmissions (Roberti, 2013). A wireless channel is defined as the path of propagation from the point of transmission to the point of reception. A wireless channel can be as simple as line of sight, in which case interference is caused by various factors, including natural terrain or artificial structures, resulting in the scattering, reflection, and diffraction of radio waves and amplification or attenuation of wireless signal power (Seidel and Rappaport, 1992). The factors influencing the strength of a wireless signal include (a) path loss, (b) slow fading, (c) shadowing effect, and (d) fast fading. Path loss is the main reason for the rapid decline of wireless signals, and it refers to the decrease in signal strength that occurs as the transmission distance increases. The shadowing effect is when a wireless signal in a wireless channel is affected by obstacles. Finally, fast fading is interference caused by a rapid decline in the coherence time.

In previous studies, wireless signal loss in wireless channels has typically been modeled through three approaches: (a) the propagation path loss model, (b) large scale propagation model, and (c) small-scale propagation model.

2.3.1. Propagation Path Loss Model

According to the theory of energy conservation, the wireless power of a radio wave is inversely proportional to the distance of propagation in a vacuum. In fact, many factors cause energy dissipation, which can occur slowly or suddenly.

The propagation path loss model includes two mathematical models: the free space propagation model and the log-distance path loss model. The free space propagation model is used to estimate the signal strength when no obstructions are present between the receiver and transmitter and where the distance between them (i.e., the Euclidean distance) is at its shortest. The free space model proposed by Friis (1946) can be used to calculate the average power received by an antenna with a given distance between transmitting and receiving antennas. The equation is expressed as follows:

$$P_r(d) = \frac{P_t G_r G_t \lambda^2}{(4\pi)^2 d^2 L} \tag{2.1}$$

where P_r denotes the transmission power at the input of the reader,P_t denotes the output power of the tag, G_r denotes the antenna gain of the reader, G_t denotes the antenna gain of the tag, λ is the wavelength, d denotes the straight line between the transmitting and receiving antenna, and L is the total signal loss. When d= 0, the received power is incalculable. Therefore, a close-in distance is usually defined as a distance approaching zero. We can use the power at $d_0$as a reference. Because $d > d_0$, a modified version of Friis'free space equation is required, as expressed in equation (2.2):

$$P_r(d) = \frac{P_t G_r G_t \lambda^2}{(4\pi)^2 d^2 L} = \frac{P_t G_r G_t \lambda^2}{(4\pi)^2 d_0^2 L} \cdot \left(\frac{d_0}{d}\right)^2 = P_r(d_0) \cdot \left(\frac{d_0}{d}\right)^2 \tag{2.2}$$

The average power of a received signal decreases with increases in distance from the transmitting antenna, which is referred to as logarithmic signal loss (Seidel and Rappaport, 1992; Scutaru and Ogrutan, 2009). The average loss power of the received signal is proportional to the *n* square of the distance, as shown in equation (2.3).

$$\overline{PL}(d) \propto \left(\frac{d}{d_0}\right)^n \tag{2.3}$$

This study adopted the log-distance path loss model to calculate the average path loss in a real space, as expressed in equation (2.4):

$$\overline{PL}(d) = \overline{PL}(d_0) + 10n \times \log\left(\frac{d}{d_0}\right) + X_\sigma \, (dB) \tag{2.4}$$

Where n denotes the path loss exponent, which indicates that the rate of path loss varies with the environment. The reference values in Table 2.2 were taken from Seidel and Rappaport (1992), where d denotes the straight line between the tag and reader, d_0 denotes the close-in distance, and X_σ denotes the interference value in the transmission space with obstructions.

Table 2.2: Value of n in Various Environments

Environment	Index n	Environments	Index n
Open space	2	Area within line of sight in building	1.6 to 1.8
Radio in urban areas	2.7 to 3.5	Shielding areas in buildings	4 to 6
Radio in urban areas with shielding effects	3 to 5	Shielded areas in factories	2 to 3

2.3.2. Large-scale Propagation Model

Large-scale propagation models are used for every type of terrain and surface feature to describe the shadowing effect of long-distance or long-duration communication signals; in the model, the shadowing effect is represented by a random variable. The shadowing effect on the received signal power following a log-normal distribution can be calculated using the path loss equation shown in equation (2.5):

$$\overline{PL}(d) = \overline{PL}(d_0) + 10n \times \log\left(\frac{d}{d_0}\right) + X_\sigma(dB) \tag{2.5}$$

The log-normal shadowing effect refers to the shadowing effect produced when the propagation distance of different paths is identical, which indicates that the radio signal path loss follows a Gaussian or normal distribution.

2.3.3. Small -Scale Propagation Model

Small-scale propagation models are used for short distances or short durations and involve rapid changes in signal loss. Such changes include the waveform phase, frequency, amplitude, and multipath phenomenon. The phenomenon results in the receiving antenna obtaining more than one signal from the transmitting antenna. The signal exhibits loss and delay; furthermore, because the transmission distance and time differ, interference to received signal occurs, resulting in signal gain or loss.

These three phenomena exist simultaneously in the wireless channel. This study adopted the log-distance path loss model to establish a mathematical model of wireless signal propagation in real 3D spaces.

2.4. Interference Problems Due to Material Composition

In equation (2.4), X_σ denotes the value of interference in a transmission space that contains obstructions. In fact, researchers have directly detected the interference value. The interference coefficient of various obstructions in a room environment, as determined by Hsu and Yuan (2011), are shown in Table 2.3.

Table 2.3: Interference Coefficient X_σ of Various Obstructions

Obstructions	Interference Coefficient X_σ	Obstructions	Interference Coefficient X_σ
Sofa	3.05	Glass windows in brick walls	2
Television	1.5	Metal framed glass wall	6
Wooden chair	4.1	Office cubicles	6
Concrete beams	0.575	Metal doors in brick walls	12.4
Sofa	3	Free Space	0

Hsu and Yuan (2011) proposed equation (2.6) for the log-distance path loss model, where D_{ij} denotes the straight line between the transmitter and receiver, sf denotes the working frequency of the wireless device, N_{gij} denotes the obstructions between the transmitter and receiver, and$L_g(D_{ij})$ denotes the interference value of the obstructions between

the transmitting and receiving antennas.

$$\overline{PL}\left(D_{ij}\right) = 10n\ log_{10}\ D_{ij} + 20\ log_{10}\ sf - 27.55 + \sum_{g=1}^{o} N_{gij} L_{g}(D_{ij}) \quad (2.6)$$

Hsu and Yuan (2011) proposed equation (2.7), wherein p is the number of materials that comprise the obstructions; MC_c denotes the interference value of the obstructions, calculated using the material composition and distance (see Tables 2.4 and 2.6 for the variable definitions), andCR_c denotes the material composition ratio (Table 2.5).

$$L_g\left(D_{ij}\right) = \sum_{c=1}^{p} \frac{MC_c CR_c}{p}) \quad (2.7)$$

Table 2.4: Distance of Interference by Materials Composition: MC_c

Material \ Distance	0–1(m)	1–2(m)	2–3(m)	3–4(m)	4–6(m)	>6(m)
Metal	Very Large	Large	Medium	Small	Very Small	Very Small
Plastic	Large	Medium	Small	Very Small	Very Small	-
Wood	Large	Medium	Small	Very Small	Very Small	-

Table 2.5: Composition Ratio: CR_c

Composition	Composition Ratio
Metal	0.6–0.8
Plastic	0.2–0.3
Wood	0.6

Table 2.6: Interference Representative Value *(dB)*

Linguistic Variable	Fuzzy Region	Representative Value
Very Small	{0,3}	1.5
Small	{1,5}	3
Medium	{3,7}	5
Large	{5,9}	7
Very Large	{8,10}	9

2.5. Multiobjective Genetic Algorithms

A heuristic algorithm can be used to conduct local or global searches to derive fitness solutions in a reasonable time (Yang et al., 2013). Heuristic algorithms include genetic algorithms (GAs), simulated annealing algorithms (Kirkpatrick et al., 1983), and particle swarm optimization (Kennedy and Eberhart, 1995), among others.

Because solving multiobjective problems is crucial, researchers have developed various multiobjective algorithms to solve them. Schaffer (1985) proposed a multiobjective evolutionary algorithm called the vector evaluated GA. Hajela and Lin (1992) proposed a GA that includes a weighting concept. Srinivas and Deb (1994) developed the nondominated sorting GA (NSGA) by increasing the scope of the solution to determine the optimal solution. Deb et al. (2002) developed the NSGA-II by adding a crowding-distance sorting mechanism to the NSGA to improve the calculation mechanism. The NSGA-II has been widely used in problem solving. Lin and Yeh (2012) combined the NSGA-II with the TOPSIS method to solve a computer networking problem.

The present study employed the NSGA-II to solve WSN planning problems and adopted the dynamic crowding distance proposed by Luo et al. (2008), and the diagram of Plato frontline distribution was integrated into the model to increase the uniformity and diversity.

3. RESEARCH METHODOLOGY

3.1. Assumptions

In this study, the assumptions for WSN planning are described as follows: (a) Environment: indoor environment. (b) The plant building contains no high-voltage processing equipment or machinery; instead, it mainly contains light industry or assembly machinery and equipment. (c) The plant building contains warehouse and production areas. (d) Because the production effect is reduced in low-altitude areas, a wireless reader cannot be deployed in low-altitude areas. (e) The detection tag's location is decided pre deployment to ensure that each location can connect. (f) The wireless devices operate on the same working frequency. (g) Electronic tags, readers, antennas and lines exhibit no hardware power dissipation. (h) The reader wireless signal geometry in space is spherical. (i) Refraction, diffraction, reflection, and multipath phenomena are ignored. (j) The reader in the deployment space can be deployed for installation and setup.

3.2. Procedure

A mathematical model based on the NSGA-II for WSN planning was developed for this study. The research process in this study was as follows: Step 1, review the literature and define the research method. Step 2, define the mathematical parameters and develop equations based on NSGA-II. Step 3, analyze scenarios and derive the conclusion. This process is depicted in Figure 3.1.

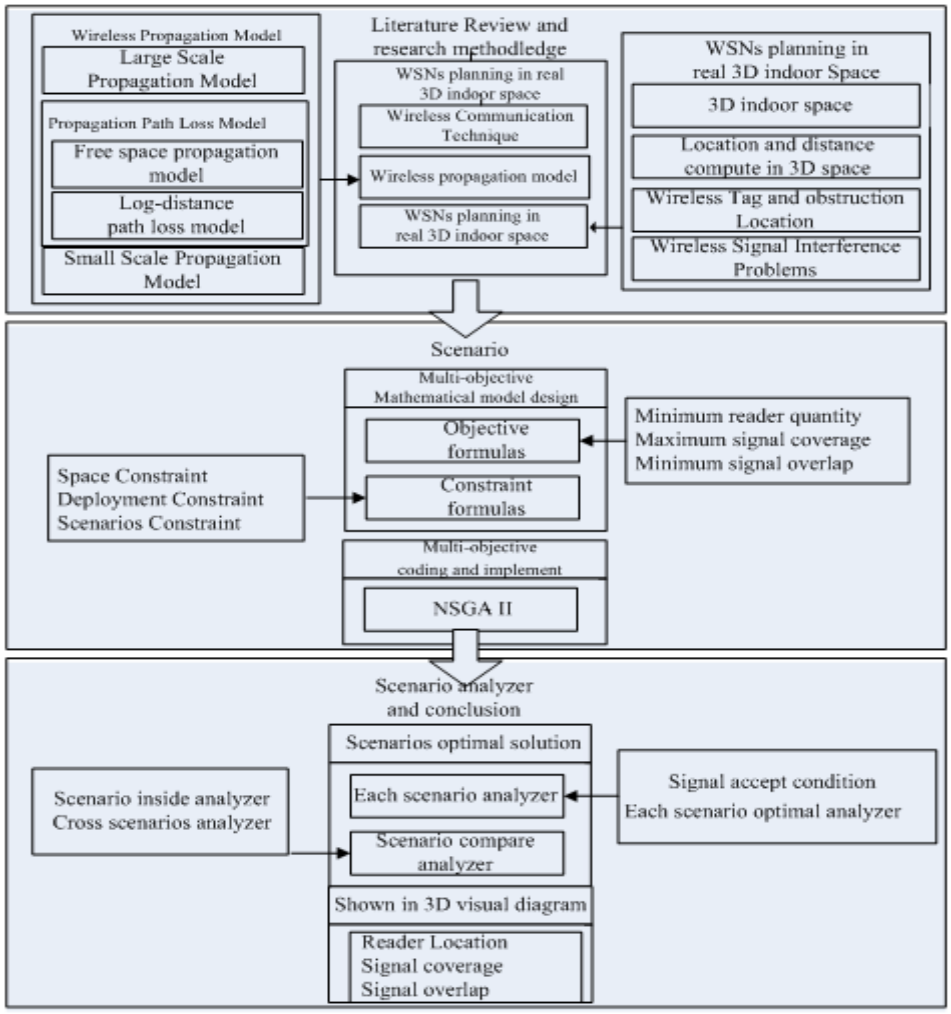

Figure 3.1: Research Procedure

3.3. Multiobjective Mathematical Model

3.3.1. Definition of Mathematical Parameters

The parameters and notations used in this study are defined in Table 3.1.

Table 3.1: Mathematical Parameters

Symbol	Description
i	Index of reader, $i \in (1,2\cdots,n)$
j	Index of tag, $j \in (1,2\cdots,m)$
g	Index of obstructions, $g \in (1,2\cdots,o)$
c	Index of materials composition, $c \in (1,2\cdots,p)$
x	x-axis
y	y-axis
z	z-axis
PG	Set of readers in available location, $PG = \{(x_c, y_c, z_c)\}$
FG	Set of readers in fail location, $FG = \{(x_c, y_c, z_c)\}$
TG	Set of tags in available location, $TG = \{(x_c, y_c, z_c)\}$
TFG	Set of tags in fail location, $TFG = \{(x_c, y_c, z_c)\}$
OG	Obstructions space
n	Number of tags
m	Number of readers
o	Number of obstructions
p	Total material composition of an obstruction
TS	Set of all tags in the warehouse area
T_i	Location (x, y, z) of tag i, $i = 1,2,\ldots,n$
RS	Set of all readers in the warehouse area
RU	At most reader quantity
RL	At least reader quantity
R_j	Location $(x, y, z)$of reader j, $j = 1,2,\ldots,m$
$\overline{PL}(D_{ij})$	Average path loss of tag i to reader j
D_{ij}	Euclid straight line distance of tag i to reader j
s	Received power threshold guaranteed reader-to-tag communication
AS_i	Set of path loss of tag i to reader j, $AS_i = \left\{R_j \middle\| R_j \in RS, and\ \overline{PL}(d_{ij}) \leq s\right\}$
sf	Working frequency (MHz) of tag TS and reader RS
C_c	Obstructions combined which material
MC_{xz}	Distance of interference of material compositions
CR_{xz}	Composition ratio
$L_g(D_{ij})$	Interference loss of obstructions of reader j to tag i
N_{gij}	Number of obstructions$g$between tag i and reader j
O_g	Item of obstructions$g$, $g = 1,2,\ldots,o$
c_i	$\begin{cases}1 & \text{Tag } i \text{ receives one reader signal, } \lvert AS_i\rvert \geq 1\\ 0 & \text{otherwise}\end{cases}$
o_i	$\begin{cases}1 & \text{Tag } i \text{ receives one more reader signal, } \lvert AS_i\rvert > 1\\ 0 & \text{otherwise}\end{cases}$

3.3.2. Definition of Mathematical Formulas

In this study, minimum reader quantity (RQ), maximum signal coverage, and minimum signal overlap were used in the objective equations. The deployment space constraint and four scenario constraints were considered in the constraint

equations. The objective, constraint, and calculation equations are described as follows:

- **Objective Formulas**

$$Max\ f_1 = \sum_{i=1}^{n} {}^{c_i}/_{n} \quad (3.1)$$

$$Min\ f_2 = \sum_{i=1}^{n} {}^{o_i}/_{n} \quad (3.2)$$

$$Min\ f_3 = m \quad (3.3)$$

- **Constraint Formulas**

$$R_j \in PG \forall j \quad (3.4)$$

$$R_j \notin FG \forall j \quad (3.5)$$

$$FG \in FG \cup R_j \forall j \quad (3.6)$$

$$T_i \in TG \forall i \quad (3.7)$$

$$TFG \in TFG \cup T_i \forall i \quad (3.8)$$

$$RD \leq m \leq RU \forall j \quad (3.9)$$

$$PG,TG 0 \leq x \leq 100, 0 \leq y \leq 35, 5 \leq z \leq 10 \quad (3.10)$$

$$FG,TFG\ 0 \leq z < 5 \quad (3.11)$$

$$OG\ 0 \leq x \leq 100, 0 \leq y \leq 20, 0 \leq z \leq 10 \quad (3.12)$$

$$O_{g,(7\times x)+k,(y),(5*z)+l} \in OG\ g = 1,2,\dots,o, x = 0,1,\dots,13, y = 0,1,\dots,20, z = 0,1, k = 5, l=1 \quad (3.13)$$

$$c_i \in \{0,1\},\ o_i \in \{0,1\} \forall i \quad (3.14)$$

$$D_{ij} = \sqrt{(T_{i,x} - R_{j,x})^2 + (T_{i,y} - R_{j,y})^2 + (T_{i,z} - R_{j,z})^2} \quad (3.15)$$

$$L_g(D_{ij}) = \sum_{c=1}^{p} \frac{MC_c CR_c}{p} \quad (3.16)$$

$$\overline{PL}(D_{ij}) = 10n\ log_{10} D_{ij} + 20\ log_{10} sf - 27.55 + \sum_{g=1}^{o} N_{gij} L_g(D_{ij}) \quad (3.17)$$

- **Scenario Formulas**

$$FGO_{g,(7\times x)+k-2} \leq FG < O_{g,(7\times x)+k+2}, x = 0,1,\dots,13, k = 5 \quad (3.18)$$

$$MC_{x1}, CR_{x1}C_1 = metal, O_{g,(7\times x)+k+2}, x = 0,1,\dots,13, k = 5 \quad (3.19)$$

$$MC_{z1}, CR_{z1}C_1 = metal\ \&\ wood, O_{g,(5*z)+l}, z = 0,1, l = 1 \quad (3.20)$$

$$MC_{x2}, CR_{z2}C_2 = plastsic, O_{g,(7\times x)+k,x=0,1,\dots,13,k=5} \quad (3.21)$$

$$MC_{z2}, CR_{z2}\ C_2 = plastic\ \&\ wood, O_{g,(5*z)+l}, z = 0,1, l = 1 \quad (3.22)$$

- **Explanation of the Formulas**

(3.1). Maximum signal coverage: the total number of tags whose signal has coverage by the deployed readers.

(3.2). Minimum signal overlap: the total number of tags covered by more than one signal.

(3.3). Minimum RQ: the total number of optimally deployed readers.

(3.4). The available location in which the reader can be deployed.

(3.5). The "fail location" in which the reader cannot be deployed.

(3.6). The "fail location" in which the reader cannot be repeatedly deployed.

(3.7). The available location in which the tag can be deployed.

(3.8). The "fail location" in which the tag cannot be repeatedly deployed.

(3.9). Limitations in the number of usable readers.

(3.10). The available size of the space.

(3.11). The fail size of the space.

(3.12). The obstruction's space.

(3.13). Each obstruction's location in the obstruction space.

(3.14). Decision variables with values of 0 or 1.

(3.15). Euclidian straight line distance.

(3.16). Interference loss caused by obstructions.

(3.17). Average path loss based on a log-distance path loss model.

(3.18). Additional fail space for scenarios.

(3.19). A vertical obstruction's location when the material used is metal.

(3.20). A horizontal obstruction's location when the material used is metal and wood.

(3.21). A vertical obstruction's location when the material used is plastic.

(3.22). A horizontal obstruction's location when the material used is plastic and wood.

4. CASE STUDY

4.1. Case Description

This study defined and designed the following detailed procedure for adopting WSN planning in real 3D indoor space environments: (a) establish the layout of the warehouse and production areas, (b) define the obstructions in the plant, (c) define the tag locations and wireless specifications, and (d) define the obstruction case design.

4.1.1. Real 3D Indoor Space Design

The size of the indoor space of the plant was 100 × 35 × 10 m. In the warehouse area, the X-axis was from 0 to 100 m, the Y-axis was from 0 to 20 m, and the Z-axis was from 0 to 10 m. In the production area, the X-axis was from 0 to 100 m, the Y-axis was from 20 to 35 m, and the Z-axis was from 0 to 10 m. The space is shown in Figure 4.1.

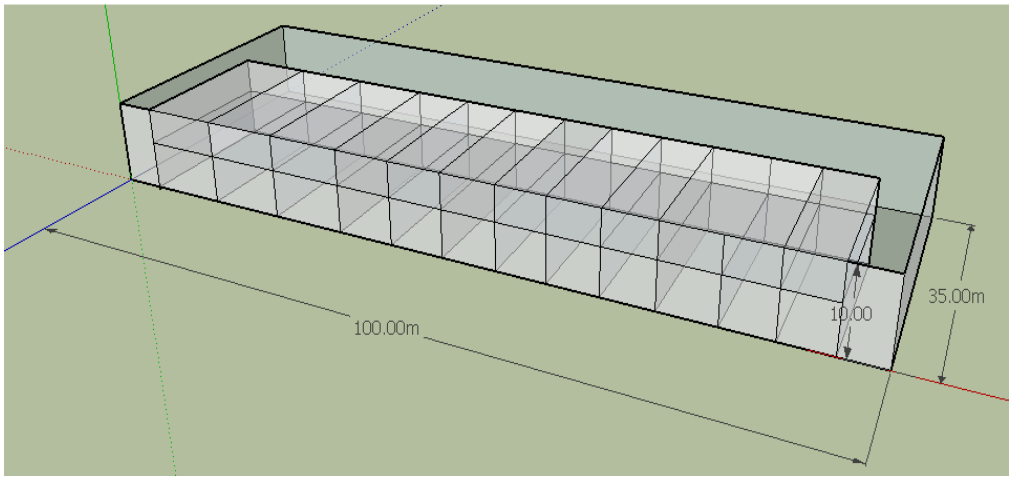

Figure 4.1: Real 3D Indoor Space

4.1.2. Plant Obstruction

All obstructions were placed in the warehouse area. The obstructions space was 91 × 20 × 10 m. Obstructions on the X-axis began at 5 m, and vertical obstructions were placed every 7 m. Obstructions on the Z-axis began at 1 m, and horizontal obstructions were placed every 5 m. The space is shown in Figure 4.1.

4.1.3. Tag Locations and Wireless Specifications

In the indoor 3D space, tags were positioned every 5 m on the X-, Y-, and Z-axes. Wireless tags were used to detect the wireless signal strength and path loss. The wireless reader and tag's working frequency was 920 MHz and adopted the IEEE 802.15.4g standard. The minimum wireless signal threshold was 49.787 dB. The wireless reader was fitted with an omnidirectional antenna. The locations and specifications are shown in Figure 4.2.

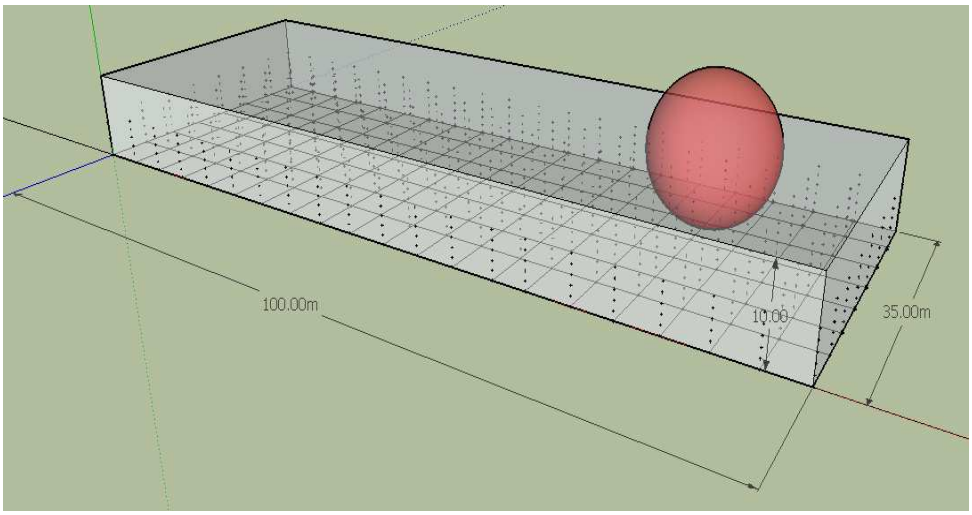

Figure 4.2: Tag location and Wireless Device Specification

4.1.4. Obstruction Scenario Design

We integrated four scenarios into our obstruction design. Vertical obstructions were either metal or plastic, whereas horizontal obstructions were either metal and wood or plastic and wood. Additionally, we implemented a deployment constraint: every vertical obstruction less than 2 m in distance cannot deploy a reader. The scenario organization and formula are shown in Table 4.1:

Table 4.1: Obstruction Scenarios

Obstruction Scenario	Material Composition		Constraint of Obstructions
	X-Axis	Z-Axis	
Scenario 1	Metal(3.19)	Metal& wood(3.20)	None
Scenario 2	Metal(3.19)	Metal& wood(3.20)	Set distance <=2 m as FG in each X-axis (3.18)
Scenario 3	Plastic(3.21)	Plastic & wood(3.22)	None
Scenario 4	Plastic(3.21)	Plastic & wood(3.22)	Set distance <=2 m as FG in each X-axis (3.18)

4.2. Experimental Design

This study employed the NSGA-II algorithm to determine the optimal solution. The parameters were population, generation, crossover rate, and mutation rate. To reduce the calculation time, Taguchi used an L9 orthogonal array in his experimental design. This study employed three levels for each factor, as illustrated in Table 4.2, and employed nine Taguchi parameter combinations (Table 4.3).

Table 4.2: Taguchi Experiment Design Parameter Levels

Parameter	Level 1	Level 2	Level 3
Generation	100	500	1000
Population	100	300	500
Crossover rate	0.6	0.8	1
Mutation rate	0.1	0.2	0.4

Table 4.3: Taguchi Experiment Design Parameter Combinations

Experiment No.	Generation	Population	Crossover	Mutation
1	100	100	0.6	0.1
2	100	300	0.8	0.2
3	100	500	1	0.4
4	500	100	0.8	0.4
5	500	300	1	0.1
6	500	500	0.6	0.2
7	1000	100	1	0.2
8	1000	300	0.6	0.4
9	1000	500	0.8	0.1

To determine the solution efficiency, Tsai et al. (2010) proposed using the maximum spread (MS), Schaffer (1985) used the number of Pareto solutions (NPS), and Veldhuizen and Lamount (1999) used the error ratio (ER). The MS and ER values were calculated using Equations (4.1) and (4.2), respectively.

$$MS = \sqrt{\sum_{m=1}^{M}(max_{i=1}^{n} f_m^i - min_{i=1}^{n} f_m^i)^2} \tag{4.1}$$

$$ER = \frac{\sum_{i=1}^{n} e_i}{n} \tag{4.2}$$

The algorithm was implemented 10 times for each parameter combination. Each scenario yielded the maximum

NPS and minimum ER as the algorithm parameters from the experimental design.

4.3. Case Study Results

The optimal parameter combination was obtained using the previously described experimental design. Each scenario's optimal result was integrated, as shown in Table 4.4. First, the NPS solution determined using the NSGA-II must fulfill the following signal condition: coverage rate (CR) of ≥0.95 and overlap rate (OR) of ≤0.2. Scenario 4 yielded 155 Level 1 solutions. Scenario 4 also attained the maximum CR and minimum OR. Scenario 3 has the lowest RQ, which was 28.

Table 4.4: Results for Scenarios 1–4

Scenario	NPS	CR	OR	RQ
Scenario 1 (S1)	81	0.982143	0.146277	31
Scenario 2 (S2)	77	0.979167	0.139785	34
Scenario 3 (S3)	105	0.988095	0.120879	28
Scenario 4 (S4)	155	0.991071	0.108635	31

Each scenario yielded the maximum NPS and minimum ER as algorithm parameters from the experimental design (Tables 4.5–4.8).

Table 4.5: Scenario 1 Results

RQ	QTY	CR	Avg. CR	OR	Avg. OR
31	9	0.964286	0.958994	0.151194	0.163728
33	5	0.964286	0.960714	0.146277	0.163577
36	4	0.964286	0.959077	0.189873	0.196347
37	10	0.967262	0.964285	0.186869	0.195804
38	23	0.98214	0.966226	0.15567	0.173365
39	1	0.958333	0.958333	0.195	0.195
41	12	0.973214	0.957341	0.160105	0.179558
42	6	0.96131	0.958333	0.193955	0.196999
44	5	0.96131	0.956547	0.181122	0.181766
48	6	0.955357	0.954365	0.181586	0.196264
Summary	81				

Table 4.6: Scenario 2 Results

RQ	QTY	CR	Avg. CR	OR	Avg. OR
34	19	0.970238	0.959743	0.139785	0.156849
36	2	0.958333	0.955357	0.177378	0.18518
37	1	0.955357	0.955357	0.185279	0.185279
40	8	0.970238	0.962797	0.164063	0.178842
43	3	0.964286	0.963294	0.178117	0.186039
44	21	0.970238	0.966411	0.159686	0.193826
45	13	0.979167	0.966117	0.144385	0.174026
47	4	0.967262	0.962797	0.179028	0.185542
49	6	0.973214	0.968253	0.183206	0.190654
Summary	77				

Table 4.7: Scenario 3 Results

RQ	QTY	CR	Avg. CR	OR	Avg. OR
28	**4**	**0.952381**	**0.952381**	**0.137466**	**0.137466**
29	1	0.955357	0.955357	0.127717	0.127717
30	1	0.952381	0.952381	0.120879	0.120879
32	12	0.967262	0.959325	0.134409	0.155439
33	3	0.952381	0.952381	0.197995	0.197995
34	10	0.96131	0.955357	0.175258	0.179407
35	58	0.988095	0.965825	0.141333	0.178432
36	1	0.952381	0.952381	0.197995	0.197995
38	3	0.973214	0.964285	0.179028	0.190539
45	7	0.988095	0.981292	0.186104	0.192102
47	5	0.964286	0.956547	0.177378	0.182071
Summary	105				

Table 4.8: Scenario 4 Results

RQ	QTY	CR	Avg. CR	OR	Avg. OR
31	7	0.964286	0.957908	0.113573	0.139162
32	16	0.973214	0.961867	0.146667	0.154211
34	7	0.973214	0.965136	0.139785	0.161874
36	7	0.964286	0.957908	0.183673	0.190976
37	50	0.991071	0.966428	0.125341	0.175839
38	7	0.964286	0.954932	0.170984	0.178063
39	9	0.973214	0.967592	0.157068	0.175751
42	3	0.96131	0.96131	0.194514	0.194514
43	13	0.97619	0.963598	0.168831	0.183837
45	11	0.967262	0.960497	0.161458	0.168474
46	1	0.952381	0.952381	0.193955	0.193955
48	2	0.952381	0.952381	0.2	0.2
49	22	0.985119	0.974702	0.108635	0.156005
Summary	155				

This study results for WSN planning are described as follows: (a) S3 NPS > S1 NPS and S4 NPS > S2 NPS: The interference value of metal is higher. (b) Results of S1 and S3: S3's optimal solutions are all superior to those of S1. Plastic is clearly more effective than is metal. (c) S4 NPS > S3 NPS: On the basis of equation (3.18), FG control should enable obtaining more solutions but would affect the optimal result. For example, S3's RQ is 28, which is less than S4's RQ of 31. (d) S1 average overlap > S2 average overlap: On the basis of equation (3.18), adjusting FG should reduce the overlap. (f) Result of S1 and S2: On the basis of equation (3.18), adjusting FG should limit the optimal solutions in the metal base of obstructions. (g) S4 CR = 0.991071, which is the optimal CR: On the basis of equation (3.18), adjusting FG should facilitate obtaining more desirable values in the plastic base of obstructions. (h) The density of the X-axis in S3 and S4 was higher than that in S1 and S2. (j) In this study, we selected S3 (RQ = 29, CR = 0.955357, and OR = 0.127717) as the optimal solution and subjected it to a detailed analysis. Figure 4.3 shows that 29 readers were deployed in the 3D indoor space. Each gray ball is a reader, and the location is shown on the right-hand side.

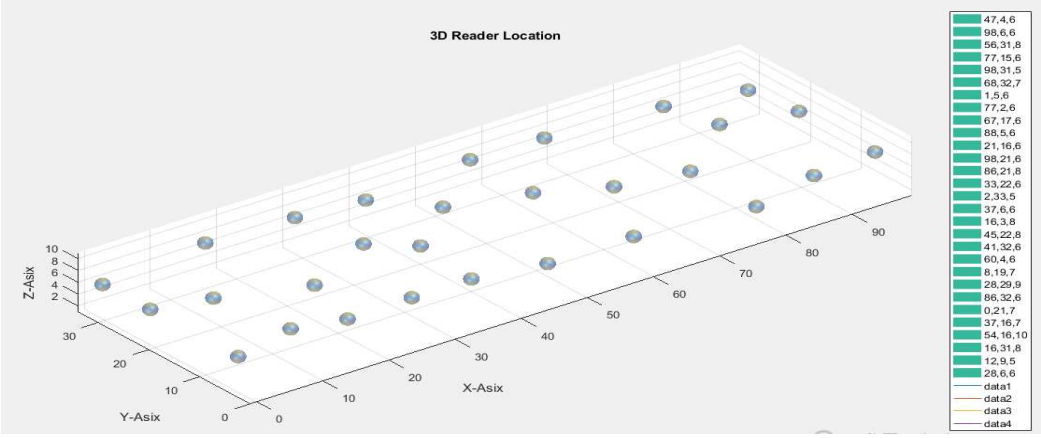

Figure 4.3: Wireless Reader Deployment in 3D Space

The wireless signal strength is depicted on the 3D contour map and 2D distribution diagram in Figure 4.4.

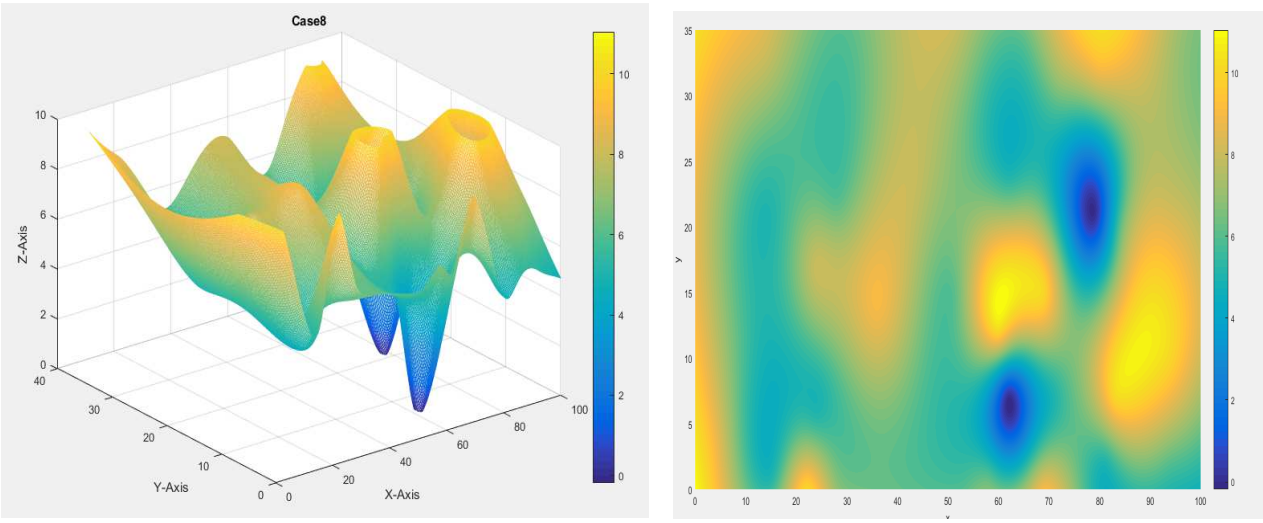

Figure 4.4: Wireless Signal Strength: 3D Contour Map, Left, and 2D Distribution Diagram, Right

On the basis of the optimal location, the 3D wireless signal coverage when deployed is shown in Figure 4.5.

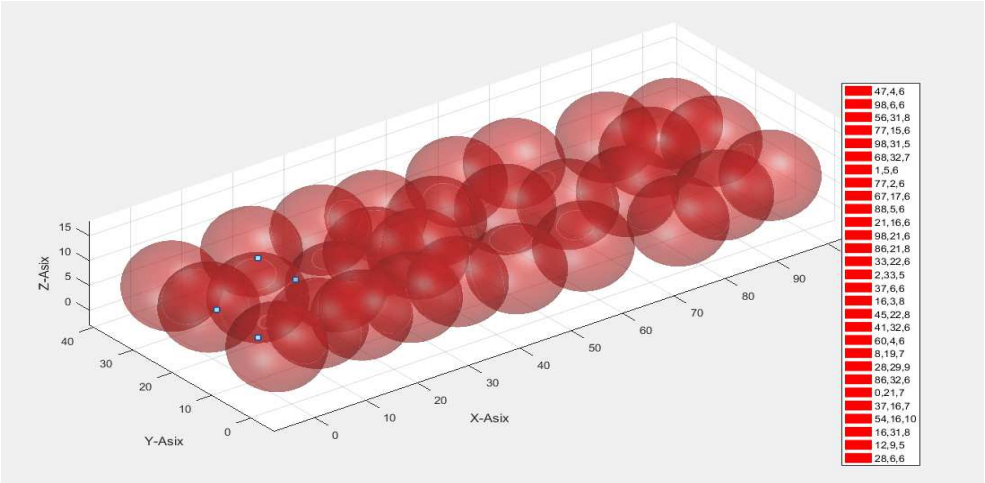

Figure 4.5: 3D Wireless Signal Coverage

Finally, the optimal deployment solution sets were clear and visible. Decision-makers can simulate altering the material of the obstructions. Find a suitable demand and exists environments optimal solution to implement.

5. CONCLUSIONS

Interference to wireless signals from obstructions is an NP-hard problem for large-space network planning. We constructed a multiobjective optimization model to assist decision-makers in WSN deployment planning. Our model can be used to reduce interference by simulating different material compositions used in existing obstructions. Decision-makers do not need to perform field measurements; our method was developed because simulating changes in the material composition of obstructions is difficult.

This study primarily investigated optimal solutions in 3D space and improved on 2D WSN planning by building a 3D space model.

The results showed that the NSGA-II is suitable for solving multiobjective problems, and all of the solutions were determined according to constraints. Compared with the obstruction scenarios, the NSGA-II yielded results that clearly converged to the Plato frontline, which may provide decision-makers with diverse solutions.

Our suggestions for mitigating interference problems in WSN deployment are as follows: (a) If possible, use plastic to replace metal, (b) combine existing metal materials with wood, (c) consider material specifications that reduce interference when building a new plant, (d) modify the available deployment space to obtain the optimal solution because spaces are not always optimally used, and (e) use the proposed model to simulate WSN planning through modifying the material composition.

The following suggestions are offered for future research:

- A plant design that increases various obstructions and conditions should be implemented.
- The purpose(s) of the physical space should be considered to determine whether CR and OR requirements differ.
- Additional situations should be investigated, such as those involving triangulation, tracking, and trace requirements.
- Additional materials and varieties of materials, such as different types of metals, should be investigated.

REFERENCES

1. *H. Gandomi, X. S. Yang, S. Talatahari, A. H. Alavi, (2013). Metaheuristic Algorithms in Modeling and Optimization. Metaheuristic Applications in Structures and Infrastructures, 1-24.*
2. *B. Luo, J. Zheng, J. Xie, J. Wu, (2008). Dynamic Crowding Distance - A new diversity maintenance strategy for MOEAS. 4th international conference on natural computation, 1, 580-585.*
3. *C. C. Chang, H. E. Tseng, L. P. Meng, (2009). Artificial immune systems for assembly sequence planning exploration. Engineering Applications of Artificial Intelligence, 22, 1218-1232.*
4. *C. C. Hsu, P. C. Yuan, (2011). The design and implementation of an intelligent deployment system for RFID readers. Expert Systems with Applications, 38, 10506-10517.*
5. *C. H. Ko, (2010). RFID 3D location sensing algorithms. Automation in Construction, 19, 588-595.*

6. *D. A. V. Veldhuizen, G. B. Lamont, (1999). Multi-objective evolutionary algorithm test suites. Proceedings of the 1999 ACM symposium on Applied computing, New York, 8, 351-357.*

7. *E. Ginters, J. Martin-Gutierrez, (2013). Low cost augmented reality and RFID application for logistics items visualization. Procedia Computer Science, 26, 3-13.*

8. *J. David Schaffer, (1985). Multiple objective optimization with vector evaluated genetic algorithms. Proceedings of the First International Conference on Genetic Algorithms, 93-100.*

9. *J. Kennedy, R. Eberhart, (1995). Particle Swarm Optimization. IEEE International Conference on Neural Networks, 4, 1942-1948.*

10. *K. Deb, A. Pratap, S. Agarwal, T. Meyarivan, (2002). A fast and elitist multi-objective genetic algorithm: NSGA-II. IEEE Transactions on Evolutionary Computation, 6, 182-197.*

11. *H. T. Friis, (1946). A Note on a Simple Transmission Formula. Proceedings of the I.R.E. and Waves and Electrons, 34, 254-256.*

12. *M. Roberti, (2013). How Can We Minimize the Failure Rate of RFID?. RFID Journal.*

13. *M. Scutaru, P. Ogrutan, (2009). High Frequency Signal attenuation Through Materials. Expert Systems with Applications, 2, 325-330.*

14. *M. Tao, S. Huang, Y. Li, M. Yan, Y. Zhou, (2015). SA-PSO based optimizing reader deployment in large-scale RFID Systems. Journal of Network and Computer Applications, 52, 90-100.*

15. *M. Younis, K. Akkaya, (2008). Strategies and techniques for node placement in wireless sensor networks: A survey. Ad Hoc Networks, 6,621-655.*

16. *N. Srinivas, K. Deb, (1994). Multiobjective optimization using nondominated sorting in genetic algorithms. Evolutionary Computation, 2, 221-248.*

17. *P. Hajela, C. Y. Lin, (1992). Genetic search strategies in multi-criteria optimal design. Structural and Multidisciplinary Optimization, 4, 99-107.*

18. *S. J. Tsai, T. Y. Sun, C. C. Liu, S. T. Hsieh, W. C. Wu, (2010). An improved multi-objective particle swarm optimizer for multi-objective problems. Expert Systems with Applications, 37, 5872-5886.*

19. *S. Kirkpatrick, G. C. Jr, M. P. Vecchi, (1983). Optimization by simulated annealing. Science, 220, 671-680.*

20. *S. Y. Seidel, T. S. Rappaport, (1992). 914 MHz Path Loss Prediction Models for Indoor Wireless Communication in Multifloored Buildings. IEEE Transaxtions on Antennas and Propagation, 40, 207-217.*

21. *W. C. Chen, P. H. Tai, W. J. Deng, L. F. Hsieh, (2008). A three-stage integrated approach for assembly sequence planning using neural networks. Expert Systems with Applications, 34, 1777-1786.*